Centre for Geo-Information

Thesis Report GIRS-2011-17

Temperature and vegetation in the Arctic: spatial variation in temporal trends

The case study of two transects in East Siberia

Loïc P. Dutrieux

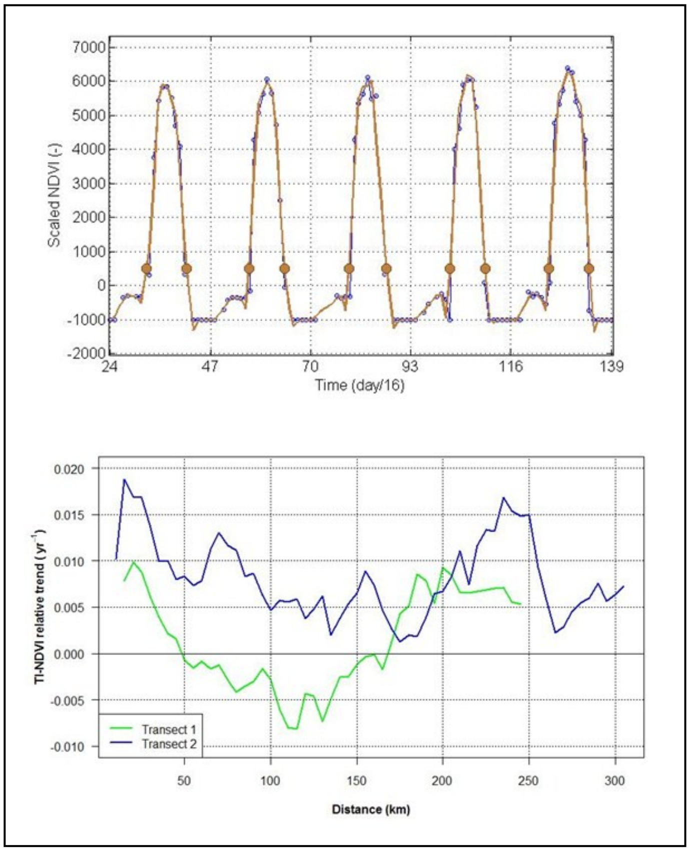

August 2011

WAGENINGEN UNIVERSITY
WAGENINGEN UR

Temperature and vegetation in the Arctic: spatial variation in temporal trends

The case study of two transects in East Siberia

Loïc P. Dutrieux

Registration number 87 11 21 205 110

<u>Supervisor</u>:

Harm Bartholomeus

A thesis submitted in partial fulfilment of the degree of Master of Science
at Wageningen University and Research Centre,
The Netherlands.

August 2011
Wageningen, The Netherlands

Thesis code number: GRS-80418
Thesis Report: GIRS-2011-17
Wageningen University and Research Centre
Laboratory of Geo-Information Science and Remote Sensing

Preface

This work originated from a thesis offer, by Harm Bartholomeus, about vegetation dynamics in the Arctic using remote sensing time series. I joined the topic, with the intention of developing my remote sensing skills, Harm Bartholomeus carrying the role of supervisor. At first the topic was broad and still opened to many approaches, but after a few meetings, we narrowed it down to what is presented in the following document. Another personal objective of this work was to improve my scientific writing skills, and eventually, depending on the quality of the output and the suitability of the results, submit the work for publication. As a consequence, Harm Bartholomeus and I agreed that the report would be written in the form of a scientific article. Although the output is in the form of a scientific article, few adjustments were made so that the work could be presented as a minor thesis and fulfill the academic requirements of the Geo-Information Science and Remote Sensing group of Wageningen University.

I would like to thank the two persons who brought an important contribution to this thesis. First, Harm Bartholomeus, who gave me enough freedom for me to develop my own ideas and provided good and useful support when it was needed. Then, Cyril Dutrieux, my brother, who had the patience to share with me his expertise in the programming domain. His help has been highly valuable to the thesis and to my personal learning of programming.

Abstract

The concern about increasing Arctic vegetation productivity has grown during the past years. Such a phenomenon has the capacity to feed back into the global climate, via its effects on permafrost thaw, and is therefore essential to be well understood. The present study analyzes, for two transects of Eastern Siberia, spatial variations in greening trend. The influence of proximity to the sea is investigated in priority, but vegetation trends are also put in relation with temperature trends. The Time Integrated Normalized Difference Vegetation Index (TI-NDVI) is used as a greenness indicator, while the Summer Warmth Index (SWI) is considered as the indicator for temperature. Both indices are derived from the Moderate Resolution Imaging Spectroradiometer (MODIS) terra sensor's NDVI and land surface temperature data, and were calculated using the TIMESAT package. Results show, for both transects, a decrease in TI-NDVI trend magnitude as distance with the sea increases, up to a distance of 50 km in one case and 120/130 km for the other. Despite this common pattern, we could not conclude on a certain effect of the proximity to the sea on the speed of the greening trend. The theory behind the sea-vegetation relations involves temperature as a driving factor of vegetation change; yet this study did not reveal any apparent relationship between SWI trend and TI-NDVI trend. A local browning trend area could also be detected for one transect while the latter is located in a generally greening area of the Arctic. This study demonstrates the capacity of relatively short time series to detect trends in TI-NDVI, and also reveals that Arctic greening is not as homogeneous as was thought. Those insights are crucial for a better understanding of vegetation dynamics in the Arctic and should be further investigated in future studies. Arctic vegetation predictions would gain in accuracy and later be used in permafrost thaw modeling studies.

Key words: SWI, TI-NDVI, MODIS, Arctic vegetation

Contents

1 Introduction

Recent warming trends have been greater over the Arctic than in average on the planet (Hansen *et al.*, 2010; Kaufman *et al.*, 2009; Serreze and Francis, 2006). These studies report an average warming 3 to 4 times higher for the Arctic than globally over the past decade. Similarly, vegetation changes have recently been observed over the Arctic. Hudson and Henry (2009), and Zhou *et al.* (2001) found that Arctic vegetation biomass tends to increase, resulting in a higher photosynthetic absorption. Many authors have demonstrated the link between the warming and the changes in vegetation recently observed (Epstein *et al.*, 2008; Hill and Henry, 2011; Olthof and Latifovic, 2007; Raynolds *et al.*, 2008; Walker *et al.*, 2006). Specifically, those changes concern an increase in plant height as well as plant biomass and modifications in plant communities composition (Chapin *et al.*, 1995; Hudson and Henry, 2009; Walker *et al.*, 2006) and are associated to an increase in photosynthetic absorption, expressed as the Normalized Difference Vegetation Index (NDVI) (Jia *et al.*, 2009; Walker *et al.*, 2009).

Such changes in Arctic vegetation characteristics may result in significant effects on both local and global climates due to complex feedback mechanisms (Chapin *et al.*, 2000; Schuur *et al.*, 2008). Arctic soils have a large carbon emission potential, which is linked to their activity (Dutta *et al.*, 2006; Von Deimling *et al.*, 2011). An increase in permafrost thaw depth will affect Arctic soils activity, and would therefore result in large carbon atmospheric emissions (Schuur *et al.*, 2008). Many authors have tried to relate vegetation change to permafrost thaw, but the answer still remains uncertain. The surface energy balance approach is often used to describe those processes. Eugster *et al.* (2000) state that due to an increase in the proportion of shrubs, regional temperature will rise due to the albedo of their canopy, lower than in the case of tundra. However, an increase in air temperature does not necessarily relate to an increase in soil temperature. Blok *et al.* (2010) showed that, due to the shading effect of their canopy, an increase in shrub cover (*B. nana*) would lead to a different partitioning of net radiations, resulting in a reduction of the ground heat flux. Summer permafrost thaw would be reduced in that case. However, *B. nana* expansion could as well have the opposite impact during winter; their snow trapping capacity providing insulation for the soils to winter temperatures (Sturm *et al.*, 2001). It is therefore essential, for climate predictions, to further understand the evolutions, under temperature changes, of vegetation in the Arctic.

Many studies have used the satellite measured NDVI as the greenness indicator for the Arctic. The index relates to photosynthetic absorption of the vegetation, and when integrated over time, provides a fair approximation of the biomass production (Reed *et al.*, 1994). Both Time Integrated NDVI (TI-NDVI) and maximum NDVI (MaxNDVI) have been widely used in Arctic vegetation studies (Stow *et al.*, 2004). TI-NDVI reflects biomass production while MaxNDVI provides information about the seasonal peak of photosynthetic absorption. Values over the Arctic range from 20 to 85 and from 0.03 to 0.70, for TI-NDVI and MaxNDVI respectively (Bhatt *et al.*, 2010; Walker *et al.*, 2005). Those indices can be investigated over several years, hence creating time series, from which trends can be derived and investigated. Various spaceborne sensors have systematically acquired spectral data of the earth surface, including the Arctic regions, hence providing time series up to 29 years in the case of the AVHRR sensors. The products, as delivered to the end users, contain already processed NDVI data, for various spatial resolutions. A very commonly used dataset in NDVI trend analysis is the Global Inventory Modeling and Mapping Studies (GIMMS) dataset (Tucker *et al.*, 2005). Derived from AVHRR sensors data acquisition, the dataset proposes a continuous time series starting in 1981, at a spatial resolution of 8 km. GIMMS data are synchronized to cope with inconsistency issues due to sensor successions. In 2000 the first of the Moderate Resolution Imaging Spectroradiometer (MODIS) sensors was launched. Although providing shorter time series, MODIS sensors have a finer spatial resolution, and are usually considered more accurate due to a narrower band sampling (Huete *et al.*, 2002). They can therefore potentially complement the long time series analysis performed at lower spatial resolution.

Using GIMMS long time series, Bhatt *et al.* (2010) have shown that proximity to the sea impacts vegetation dynamics in the Arctic regions. The mechanism can be explained by the impact summer sea ice has on near shore land temperature and hence on vegetation. Although Bhatt *et al.* (2010) noticed differences regarding the effect of sea ice on TI-NDVI between near shore areas and the full tundra domain, the relation between sea distance and Arctic vegetation productivity has not been established yet.

Based on the assumption that the greening rate, defined as the TI-NDVI temporal trend, is influenced by the proximity of the sea, this research investigates TI-NDVI trends as well as TI-NDVI/SWI trends relations along two transects in east Siberia (north-east of the Sakha Republic). The analysis is done over a time period of 11 years (2000-2010) using satellite data alone, derived from MODIS. The two main objectives of the research are: [1] Investigate the variations in greening trend, expressed as the trend in TI-NDVI, along two Arctic transects located in northern Russia. [2] Investigate the relations between SWI trend and NDVI trend along the same transects.

2 Material and Methods

2.1 Study area

We selected two transects going across the Arctic from north to south. Both transects begin near the sea shore and end at the southern limit of the circumpolar Arctic region, as defined by the Circumpolar Arctic Vegetation Map (CAVM) team (Walker *et al.*, 2005). When using the same naming convention as Bhatt *et al.* (2010), for which Arctic regions are associated with the sea they are facing, transect one belongs to the "East Siberian sea" region, while transect two is between "Laptev sea" and "East Siberian sea" regions. The coordinates of the transects are;

Upper Left corners: 71.16°, 155.69° and 72.76°, 143.19° for transects one and two respectively. Lower Right corners: 68.98°, 155.97° and 70.05°, 143.56° for transects one and two respectively. The transects strips are 25 km wide, and 243 and 302 km long for the transects one and two respectively (Figure 1).

As there was an assumption that distance from the sea, due to the impact of summer sea ice decline on local climate, would have an important effect on the vegetation trend, the transects locations were selected going directly inland, rather than going over a peninsula for instance. That way, distance from the north side of the transect directly relates to the shore distance. Similarly the transects were selected on homogeneous landscape area. In both cases, the entire transect belongs to the plain category (Walker *et al.*, 2005) and its elevation does not exceed 50 m above sea level, except for the extreme south of transect 2. Three different vegetation classes, as defined by the CAVM map, are present in transect 1 and four in transect 2, two of them (the most represented) being common to both transects (Table 1). These two categories are non-tussock sedge, dwarf-shrub, moss tundra and tussock sedge, dwarf-shrub, moss tundra.

Table 1: Vegetation classes present in the transect and their respective area.

CAVM code	Vegetation type	Area (km^2)		Relative area (%)	
		Transect 1	Transect 2	Transect 1	Transect 2
G2	Graminoid, prostrate dwarf-shrub, forb tundra	589	-	9.7	-
G3	Nontussock sedge, dwarf-shrub, moss tundra	1268	1984	20.9	49.6
G4	Tussock-sedge, dwarf-shrub, moss tundra	3707	3744	61	49.6
W1	Sedge/grass, moss wetland	-	701	-	9.3
W2	Sedge, moss, dwarf-shrub wetland	-	191	-	2.5
-	Water	496	930	8.2	12.4

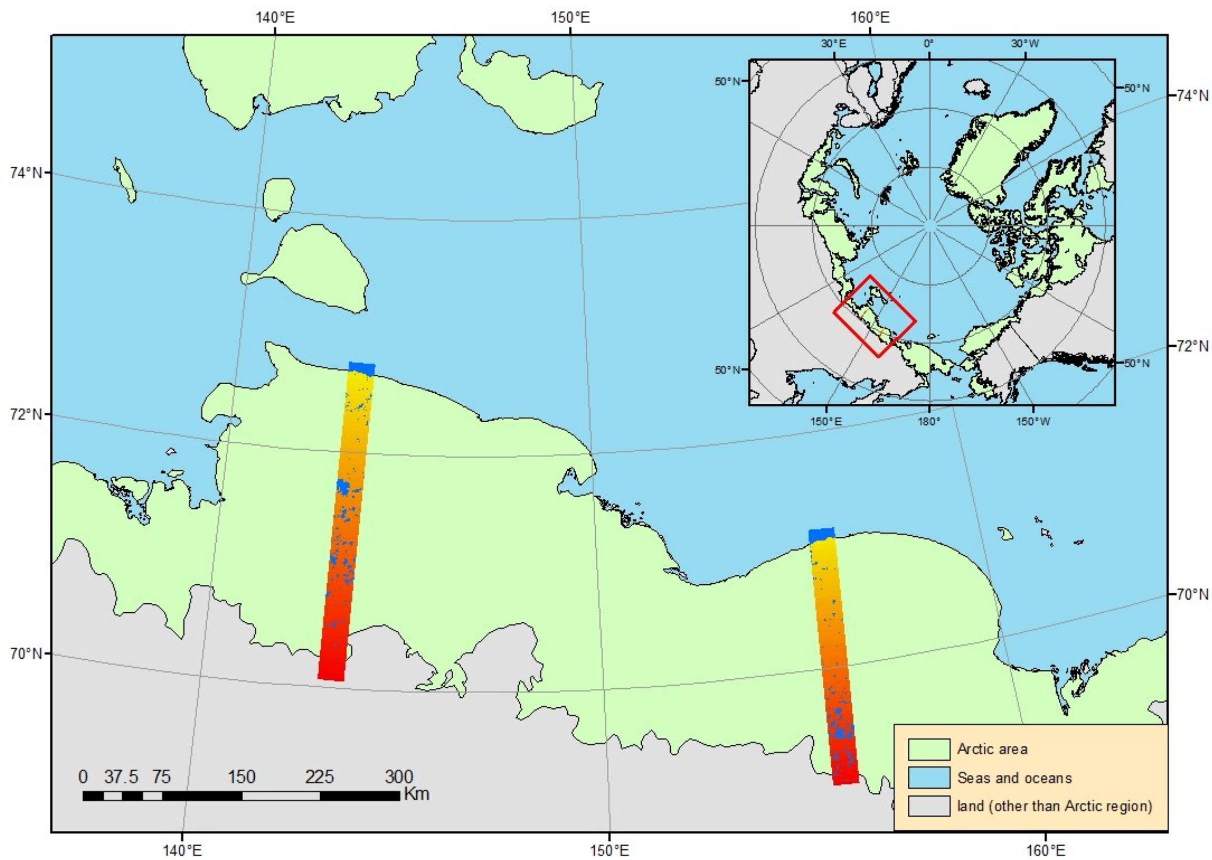

Figure 1: Location of the studied transects. The color gradient of the transects display the relative distance from their north side.

2.2 Data description

MODIS

MODIS data have been acquired since 2000, with the launch of the first MODIS sensor, on board of the Terra satellite. The sensor acquires data on a daily basis. Raw data and composite products are available at different resolutions. Data, from February 2000 until near real time acquisition can be downloaded at no costs through the United States Geological Survey Distributed Active Archive Center (USGS-DAAC)[1]. NDVI is available, already processed, in the form of 16 day data composites and Land Surface Temperature in the form of 8 day data composites. Both products were downloaded for the 1 km spatial resolution. All MODIS data used for this study are listed in Table 2.

[1] https://lpdaac.usgs.gov/

Data composites combine in one tile the pixels with the highest value over the considered period. This way, clouded pixels are, in most cases, filtered out, and cloud free composites can be delivered.

A second MODIS sensor, on board of the Aqua satellite, was launched in 2002 and started acquiring data in July of the same year. For this study, data from the Terra sensor alone were used, since they provide longer time series.

Table 2: Inventory of remote sensing data used for the study.

Product name	Product description	Sensor	Period considered	Spatial resolution
MOD13A2	Vegetation Indices	Terra	2000-2010	1000 m
MOD11A2	Land Surface Temperature & Emissivity	Terra	2000-2010	1000 m
MOD12Q1	Land Cover Type	Terra	2004	1000 m

MODIS land cover type is an annual product providing a worldwide vegetation classification at a resolution of 1 km. The product from the year 2004 was used as a water mask, to automatically exclude water pixels from the processing and analysis. The land classes other than water were not considered, as a more specific map is available for the Arctic. This circumpolar Arctic vegetation map, produced by the CAVM team (Walker *et al.*, 2005) and that distinguishes 15 floristic provinces for the whole Arctic, was used for vegetation specific analyses in this study.

TI-NDVI and SWI

NDVI is a vegetation index providing a relative estimate of the vegetation photosynthetic absorption. It is calculated as NDVI = (NIR - RED)/(NIR + RED), where NIR and RED are the surface reflectance ($W.m^{-2}$) for the Near Infrared and Red spectra respectively. NIR corresponds to wave lengths from 0.841 to 0.876 µm and RED from 0.620 to 0.670 µm. By construction NDVI varies between -1 and 1. Green vegetation tends to have a high absorption in the red and a high reflectance in the near infra-red, hence the greener the vegetation, the higher the NDVI. However, the background also influences the index, wet soils and plants growing in water for instance usually present lower NDVI values for the same photosynthetic absorption , due to the high absorption properties of water (Qi *et al.*, 1994). Such a consideration is particularly important in the case of the Arctic, where a diversity exists in the soil-plant configurations, including wetlands.

TI-NDVI is an integrated product of the NDVI. It reflects the total cumulated photosynthetic energy absorbed over a year (Reed *et al.*, 1994). It takes into consideration both length of the growing season and peak NDVI value. A base level of NDVI = 0.05 is used in the integration, to obtain TI-NDVI. Similarly, SWI, defined as the total beneficial heat energy accumulated by the plants to achieve their growing cycle, was used. Both indices have been jointly used extensively in Arctic vegetation studies, and their relation many times emphasized. Bhatt *et al.* (2010) report a strong correlation (r^2 = 0.57) between SWI and TI-NDVI overall for the Arctic. SWI is calculated as the time integral of the land surface temperature above freezing, and it is therefore expressed in Growing Degree Days (GDD).

2.3 Pre-processing

After downloading the images (MODIS tiles h22v01, h23v01, and h23v02) the tiles were mosaicked, re-projected and subsetted using the MODIS Reprojection Tool (MRT). The two subsets created correspond to the transects, so further processing could be restricted to these areas. MRT is provided by the National Aeronautic and Space Administration (NASA), and can be downloaded at no costs through the USGS-DAAC. The software allows MODIS images to be pre-processed in batch process and the output options include several formats and projections.

The TIMESAT package (version 3.0) was used to generate TI-NDVI and SWI data from NDVI and land surface temperature time series (Jönsson and Eklundh, 2004). Freely available for non-commercial academic research, the TIMESAT package was designed for analyzing time series in remote sensing data. Series with periodicity such as temperature and NDVI can be fitted using different fitting functions and several outputs can be derived from the fitting (Jönsson and Eklundh, 2002). Such method, using fitting, allows the noise captured by the sensors to be corrected. Given the short duration of the growing season in the Arctic, with sudden increase in photosynthetic activity as soon as the snow melts, the noise captured by the sensors when measuring NDVI can easily become a large part of the overall season TI-NDVI. The fitting options available in the version 3.0 of TIMESAT include Savitzky-Golay filter, least-squares fitted asymmetric Gaussian or double logistic smooth functions. Outputs are presented in the form of seasonality parameters, hence providing, on a pixel basis, one value per season and per parameter. Both TI-NDVI and SWI are represented by the small integral, which is, for a given year, the integral between base levels, mentioned earlier, and the fitted curve. The TIMESAT outputs were imported and analyzed into the R statistical software (R Development Core Team, 2011).

2.4 Analysis

Relative trends were calculated on a pixel basis from the TIMESAT output, this latter providing one value for TI-NDVI as well as one for SWI per pixel and per year. The relative trends are defined by the slope of the linear regression of the time series, divided by the mean of the variable, calculated over the 11 years of MODIS observation. Using relative instead of absolute trends allows comparison between variables having different dimensions; TI-NDVI and SWI in this case. In addition to the calculations on a pixel basis, the values were averaged by five km distance classes so that profiles along the transects could be represented.

In order to explain variations in TI-NDVI relative trends, linear regressions were performed, with SWI trends. The SWI trend/TI-NDVI trend relation emphasizes the importance of the magnitude in SWI change on the magnitude of TI-NDVI change. For all regressions, a Pearson coefficient of determination was calculated.

3 Results

3.1 Pre-processing

The TIMESAT package was used for fitting both NDVI and land surface temperature time series, and, from these fitting, to calculate TI-NDVI and SWI for each year, on a pixel basis. Figure 2 depicts the three fitting options available in the software applied to a random NDVI pixel of transect 1.

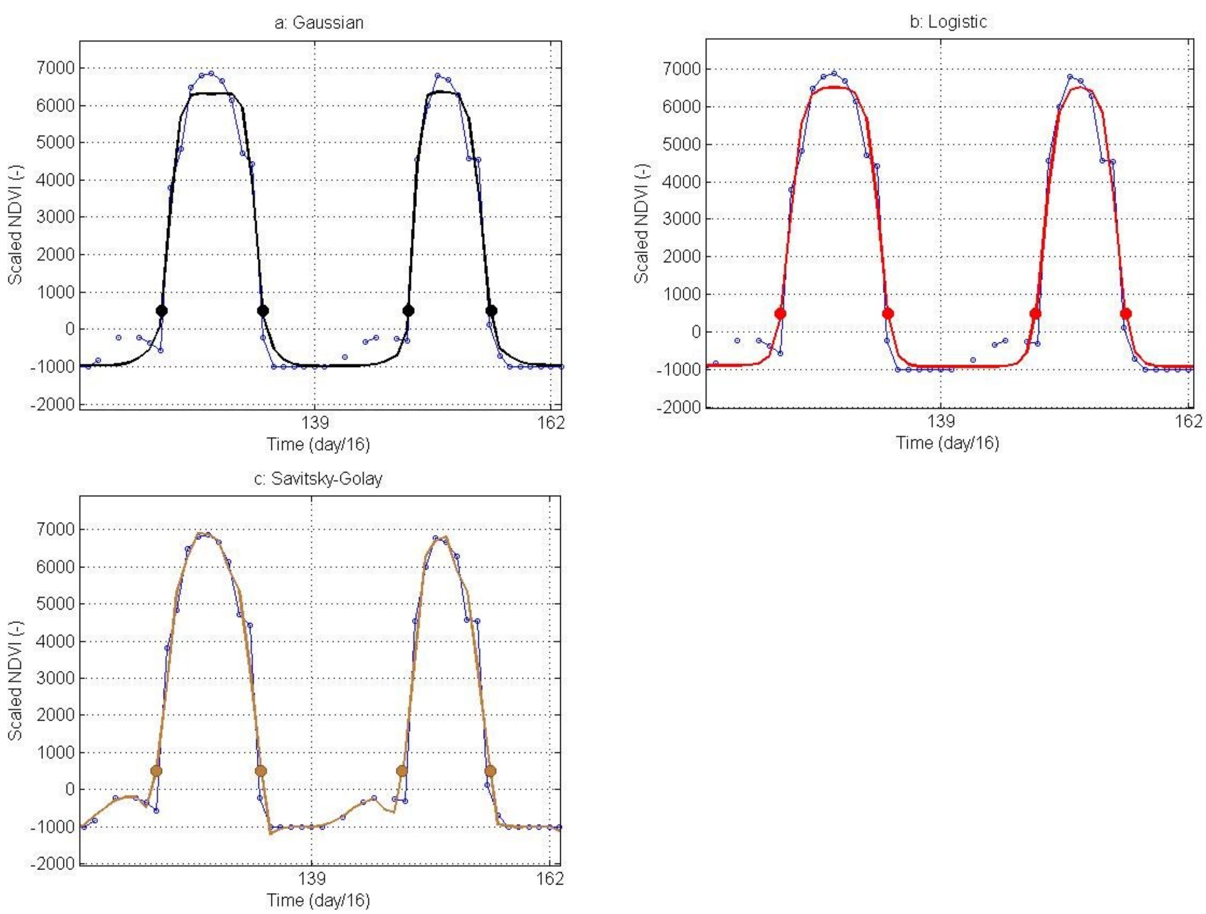

Figure 2: Preview of the 3 fitting functions available in TIMESAT, applied to two seasons, for a random NDVI pixel of transect 1. The dots at y = 500 represent season starting and stopping points, used as base level in the integration.

As snow is covering the Arctic during the major part of the year, vegetation cycles are characterized by short duration growing seasons and sudden increases in photosynthetic activity as soon as the snow melts. The best method to model the season given the non-continuity of the photosynthetic absorption signal was found to be using the Savitzky-Golay function. Similar observation can be made regarding temperature, and both TI-NDVI and SWI could thus be calculated following this method.

3.2 TI-NDVI and SWI, overall ranges

The TI-NDVI and SWI were averaged over the 11 years of MODIS observation, per pixel and for 5 km distance classes. The results are presented in Figure 3. Values measured over the transects range from (defined as the 5 and 95 percentiles of the entire range) 42.4 to 74.3 and from 1100 GDD to 1950 GDD for TI-NDVI and SWI respectively. Those ranges do not strongly vary between the two transects, which partly confirms the environmental similarity between them. The values corroborate well with values measured by Walker *et al.* (2009), and Bhatt *et al.* (2010). Ranges of 300 GDD to 1500 GDD (10 °C mo – 50 °C mo) for SWI, were presented in a study over the Yamal peninsula (West Kara sea), while mean TI-NDVI values reported for the different Arctic regions range between 30 and 90.

After a first observation of the spatial distribution of both variables, one can say that in all four cases (average TI-NDVI and average SWI for transects 1 and 2) the variables are spatially structured. Both variables tend to increase when going toward the south. This observation is confirmed by the linear regressions performed on the profiles (dashed line in Figure 3). In both transects and for both average TI-NDVI and average SWI, the linear regression presents an increase in the southward direction.

The fitting of the linear model to the distance profiles is good in all four cases. Thus, beside local variability, average TI-NDVI and SWI can be described as a linear function of the latitude. The highest local variability seems to appear for the first transect, between 180 and 200 km. At this location, the profiles are 200 GDD and 8 TI-NDVI units lower than their respective linear models. From the juxtaposed map, this area appears as well to have the highest inland water density of all the transect. A similar phenomenon does not seem to appear in the case of the transect 2, for which inland water density also appears to be high in some locations. Therefore, it is not possible to conclude on a direct effect of inland water on TI-NDVI and SWI for the Arctic. Furthermore, a mixed pixel effect, due to this dense lake network, is not to exclude, for explaining such local variations in TI-NDVI and SWI. Pixels with mixed signal including water would present lower values for both variables.

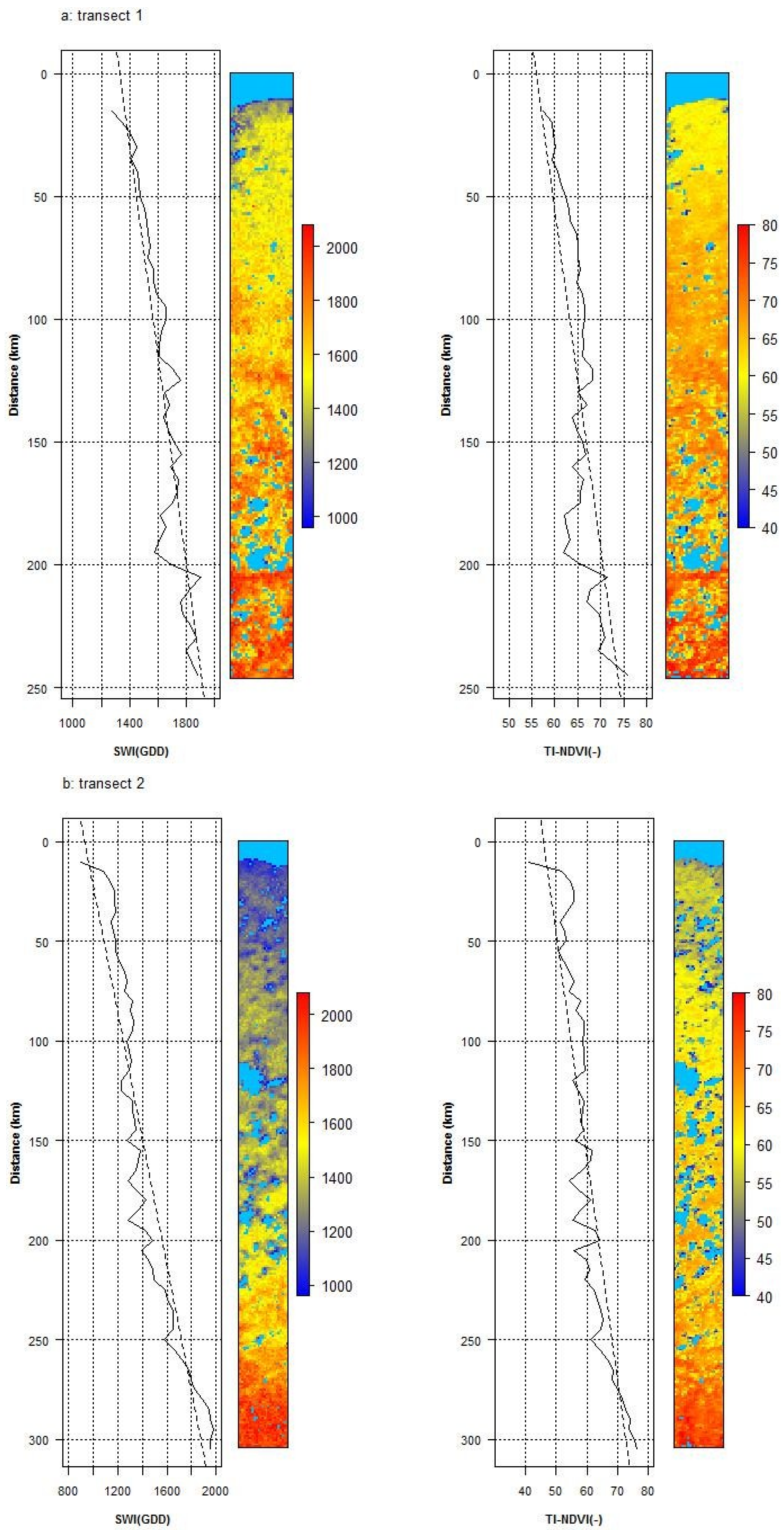

Figure 3: Map depicting TI-NDVI (right) and SWI (left), both averaged over the 11 years of observation of MODIS Terra between 2000 and 2010 for transect 1 (a) and transect 2 (b). The profiles show the average pixel values per 5 km distance classes.

The relation between average SWI and average TI-NDVI is confirmed by strong correlation between those two variables (appendix 1) with $r^2 = 0.53$ and $r^2 = 0.6$ for transect 1 and transect 2 respectively and both correlations significant ($p < 0.001$). The strength of this relation appears to have constancy over the Arctic; Bhatt *et al.* (2010) reported values of $r^2 = 0.57$ for the same regression. Such high correlations indicate that SWI is an important driver for the establishment of vegetation in the Arctic.

3.3 TI-NDVI and SWI trend patterns and relations

Relative trends were computed for both TI-NDVI and SWI, considering the 11 years of MODIS observation, on a pixel level and per 5 km distance classes. The trend maps, significance of the trend and trend profiles along the transects are presented, for both transects, in Figure 4.

Regarding TI-NDVI relative trend profile for transect 1, a negative pattern can be observed in the higher part of the transect, with TI-NDVI relative trend decreasing when going farther from the north side of the transect. The trend, starting positive near the sea shore, turns negative from a distance of 50 km. In this section, we therefore do not observe a greening trend anymore, but a decrease in vegetation instead. A minimum is reached at a distance of about 120 km, then the trend starts increasing again, although it remains negative up to a distance of 160 km. Transect 1 profile is therefore characterized by a section of about 100 km presenting a negative trend. As opposed to transect 1, transect 2 depicts a constantly positive TI-NDVI relative trend. TI-NDVI relative trend values range (5 and 95 percentiles of the entire range) from -0.01 yr^{-1} to 0.013 yr^{-1} and from -0.002 yr^{-1} to 0.019 yr^{-1} for transects 1 and 2 respectively. In both cases, the type of vegetation (depicted by the colored bars on the left side of the profiles) does not seem to strongly influence the greening trend as we do not observe sharp patterns in the trends near vegetation classes boundaries. Only few pixels present significant relative TI-NDVI trends; 0.7 % and 5.2 % of the land surface for transects 1 and 2 respectively are significant at the 95% confidence interval. However, the existence of visual spatial patterns for TI-NDVI trends makes us believe that, even though trends are not statistically significant, they are not random either. This lack of validation via statistics may be a consequence of the length of the time series, including only 11 years.

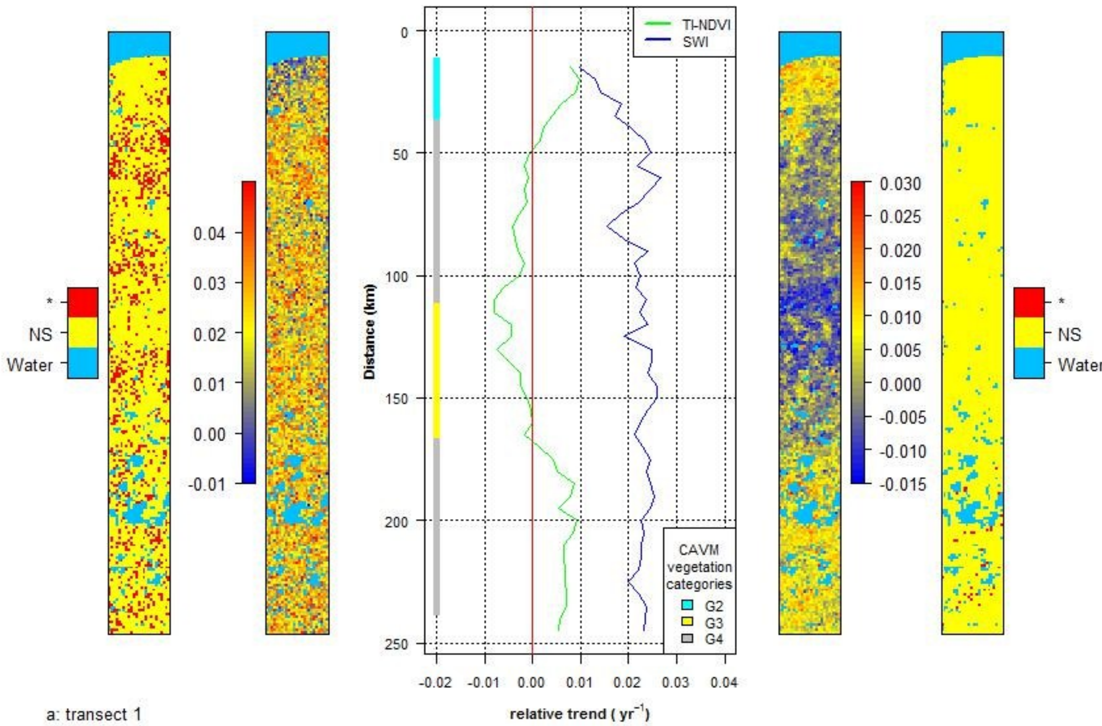

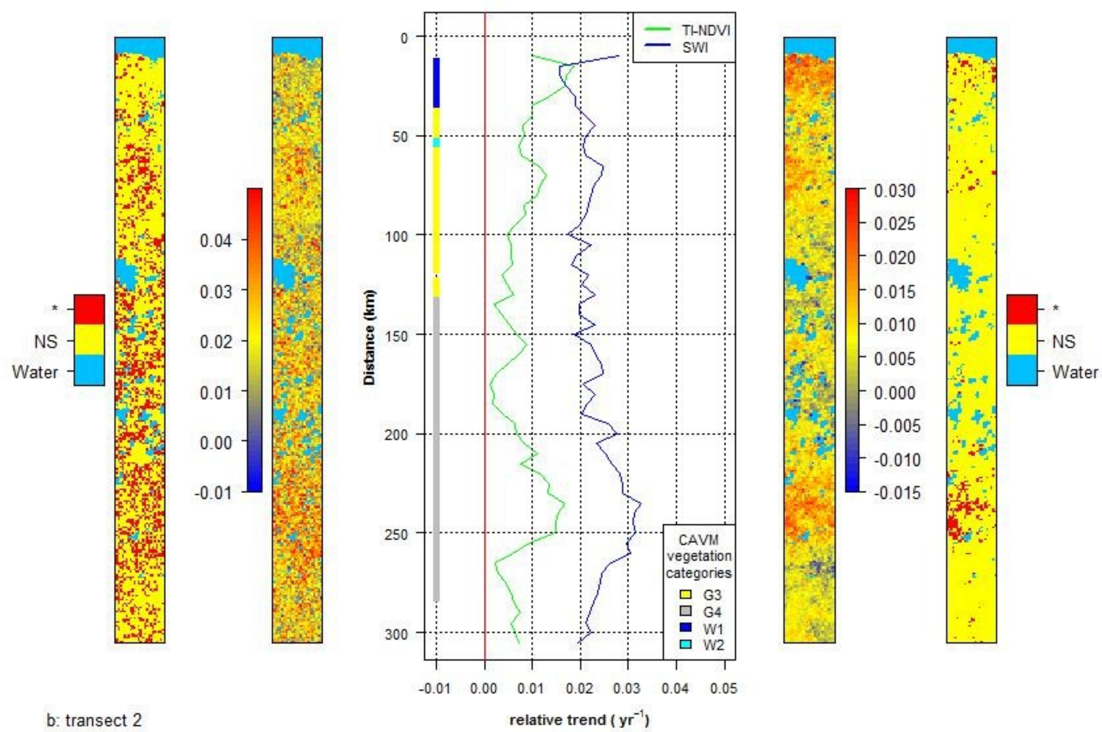

Figure 4: SWI relative trend and significance levels maps (left), TI-NDVI trends and their significance levels maps (right), and distance profiles of both SWI and TI-NDVI trends (center); for transect 1 (a) and transect 2 (b). The profiles show the average pixel values per 5 km distance classes.

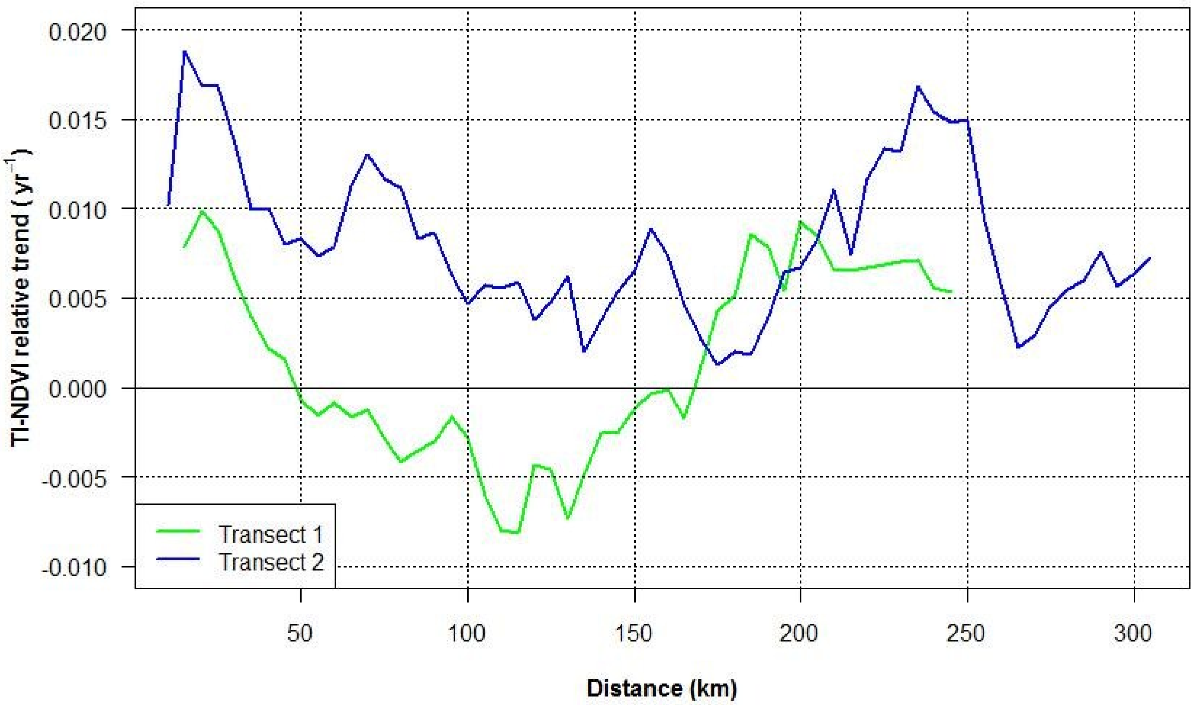

Figure 5: TI-NDVI trend profiles of transects 1 and transect 2. The profiles were made by averaging all pixels trend values per five km distance classes.

TI-NDVI in relation with distance from the north side of the transect was compared for the two transects (Figure 5). Despite local fluctuations, a downward trend can be observed in both cases for the first part of the profile. Then both profiles tend to either stabilize, in the case of transect two, or start increasing, for transect one, from a distance of 120/130 km from the sea shore. After this turning point, no common pattern can be distinguished between the two transects. Whether this common pattern, in the first 120/130 km, can be attributed to the effect of proximity to the sea is not known. The indirect effect of sea ice concentration on vegetation concerns a cooling effect of ice on land temperature. Yet the land temperature trend, as shown in Figure 4, appears to diverge from the TI-NDVI trend; at least in this first section of the transects.

Although the TI-NDVI relative trends present similar patterns between 0 and 120/130 km for the two transects, when considered, the values are different. In the case of transect 2, the trend remains always positive, with a minimum of about 0.002 yr^{-1}, while the trend is negative for transect 1 between 50 and 170 km, with a minimum of about -0.008 yr^{-1}.

A first observation about the SWI relative trends concerns the lack of spatial structure. While patterns can be observed on the transect maps for TI-NDVI relative trends, the SWI relative trend maps appear to be noisy. Such high local variability for a variable like temperature is surprising and therefore raises the question of the relevance of studying temperature at a relatively fine (1 km) spatial resolution. Despite this higher noise level, more pixels present a significant trend than in the case of TI-NDVI relative trend. 17.1 % and 27.2 % of land pixels present a significant trend at the 95% confidence interval for transect 1 and transect 2 respectively. When considering the profiles, for both transects SWI is rather stable, with values ranging around 0.02 yr^{-1}, and local extremums to 0.03 yr^{-1} and 0.01 yr^{-1}. Only in the first 50 km of transect 1, SWI relative trend appears to be increasing. This could be due to a buffer effect of remaining summer sea ice near this location, even though recent mappings suggest that this region of the Arctic was particularly concerned with sea ice retreat during the past few years (Comiso *et al.*, 2008). Although the correlation is well established between summer sea ice concentration and temperature (Bhatt *et al.*, 2008), we cannot be certain that the SWI trend pattern observed in the north of transect one is linked to summer sea ice. Furthermore, the same pattern can hardly be seen in the case of transect 2, whereas distance between the two transects does not exceed 450 km.

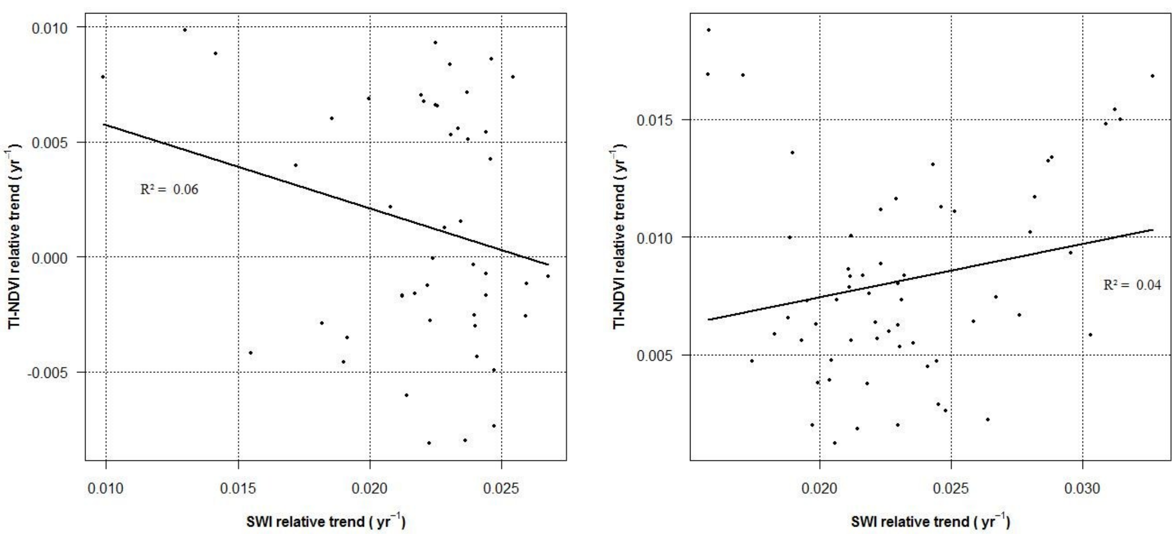

Figure 6: Relationship between SWI and TI-NDVI relative trends for transects 1 (left) and 2 (right). Each value represents the average trend per 5 km distance classes.

Visually, the relationship between SWI and TI-NDVI relative trends appears to be stronger in the case of transect 2 than for transect 1 (Figure 4). Both curves present similar patterns for transect 2, while they diverge for transect 1. This observation is confirmed by the simple linear regression analysis performed between TI-NDVI and SWI relative trends. Figure 6 presents for each transect separately the regressions performed at the 5 km distance classes scale, while Figure 7 and Figure 8 present the results at the pixel level, for each vegetation class. Confirming the visual interpretation from the profiles, the relations are generally stronger, with slightly higher coefficients of determination, for transect 2 than for transect 1. At the pixel level, coefficients of determinations do not exceed $6x10^{-4}$ for transect 1, whereas in the case of transect 2, and for all four vegetation classes, r^2 is always higher than 0.01. The highest coefficients of determination found concern the vegetation class Sedge, moss, dwarf-shrub wetland, in transect 2, with a value 0.04 and a positive correlation. Correlations for transect 2, at the pixel level, are constantly significant for $p < 0.01$, and even $p < 0.001$ in the case of two vegetation classes. Even though the results of the correlation tests show that the relationships appear to be stronger in one case, and present constant significance for transect 2, the relationships between trends remain weak in general, and SWI trends seem to have little to no influence on TI-NDVI trends. The high significance observed can only be attributed to the large number of observations. Such relationships, highly significant, but with little strength, even though validated by statistics, reveal a dependance between the variables, but of such weakness that it hardly has any practical implications.

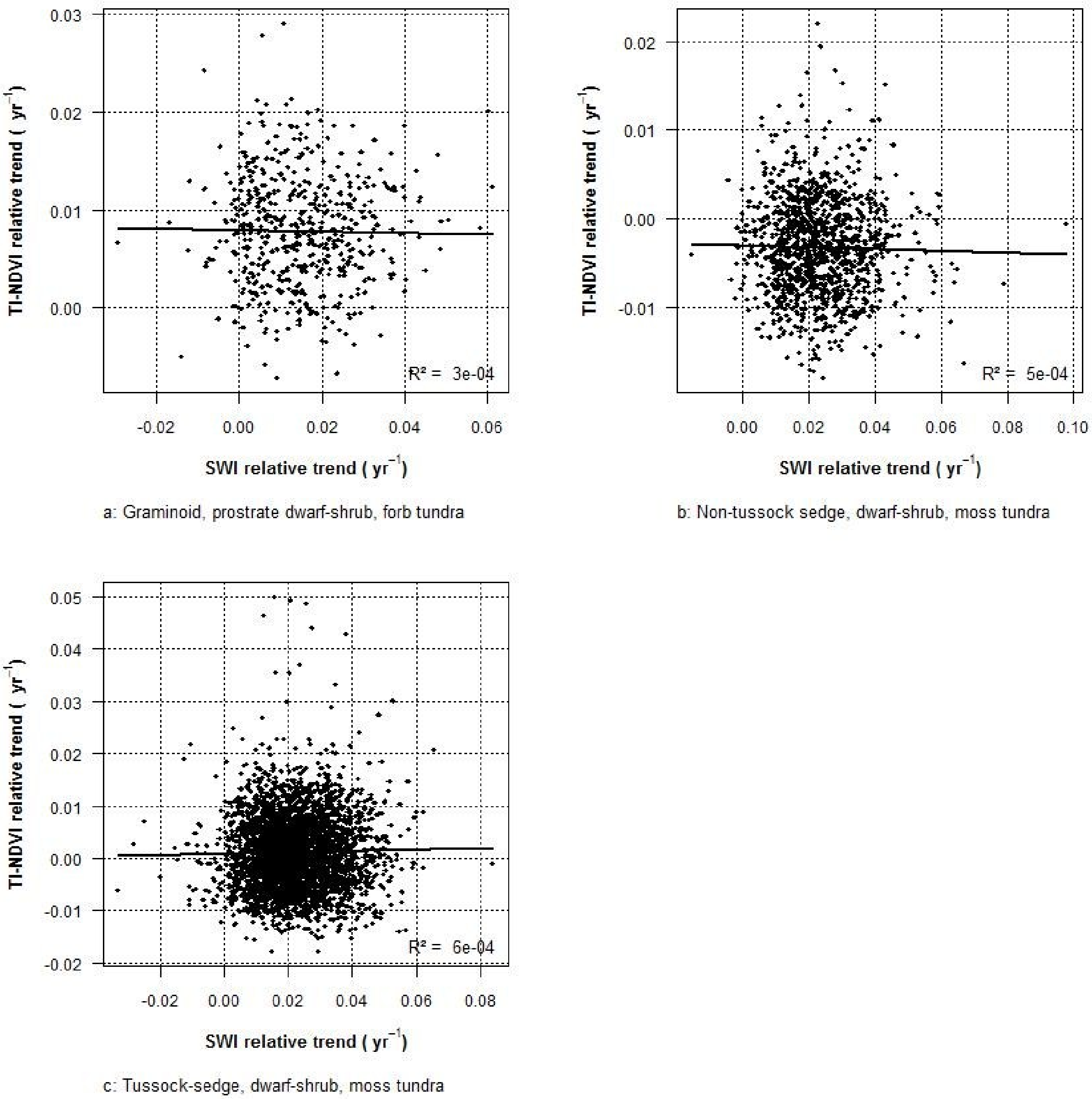

Figure 7: Relationships per vegetation classes for transect 1 between SWI trend and TI-NDVI trend, on a pixel basis.

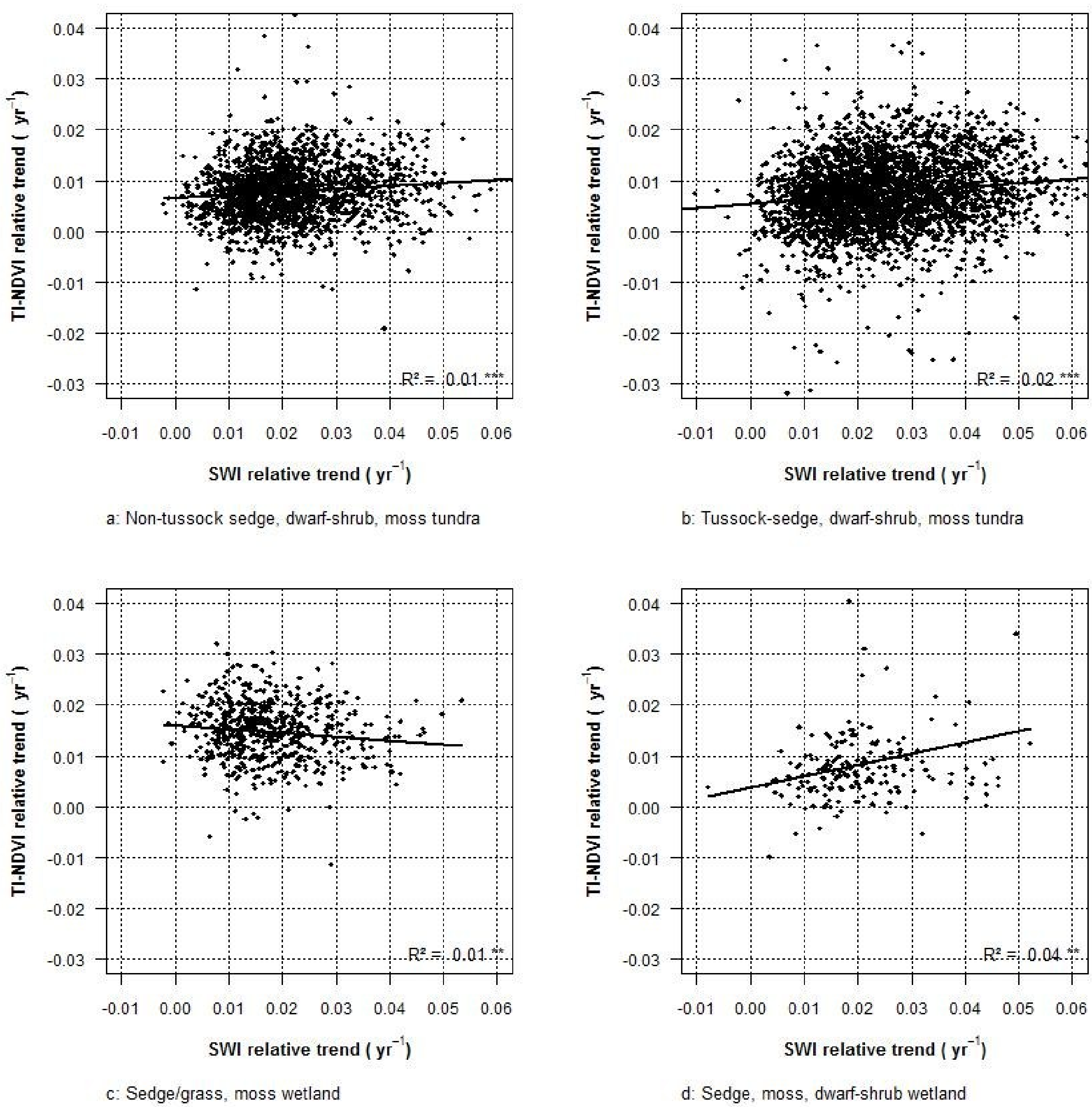

Figure 8: Relationships per vegetation classes for transect 2 between SWI trend and TI-NDVI trend, on a pixel basis.

4 Discussion

In this study, vegetation trends along two transects of east Siberia were investigated. Both transects were departing from the coast and going inland in a southward direction. Spatial variations in greening trends of Arctic vegetation could be investigated, and particularly the effect of proximity to the sea. According to authors' knowledge, only one study considered distance to the sea in a vegetation trend analysis (Bhatt *et al.*, 2010). The study came to the conclusion that vegetation change, expressed as change in TI-NDVI, is linked to sea ice decline, via a faster warming for near ice retreat area than for other areas. However, the relation between distance to the sea and change in TI-NDVI was not characterized. The present study was then conducted to gain further insight into this, still uncertain, interaction between summer sea ice decline and vegetation dynamics. TI-NDVI was used as the vegetation production indicator and SWI as the heat parameter. TI-NDVI trends, as well as their relation with SWI trends, were analyzed and compared for the two transects.

NDVI and land surface temperature time series from MODIS terra sensor were used to derive TI-NDVI and SWI, hence working with 11 years' time series (2000-2010). Because Arctic vegetation seasons are singular, characterized by short growing periods between the time snow melts in spring and new snow falls in fall, we decided to calculate both TI-NDVI and SWI via curve modeling. The TIMESAT package was used for this purpose (Jönsson and Eklundh, 2004). We believed that sensor's noise could have a large influence when integrating both NDVI and land surface temperature; curve modeling was then a way to reduce this noise. Comparisons between ranges found in this study using modeled curve integral method and simple summing of bi-weekly data as performed in most studies do not reveal large differences (Bhatt *et al.*, 2010; Walker *et al.*, 2009). The relevance of using such a method, more complicated, and involving more variables is therefore questioned.

On average, for both transects, there is a greening happening over the 11 years of MODIS observation. These values tend to be higher than what has been observed previously for this region of the Arctic. Relative trends of 0.0011 yr^{-1} and 0.008 yr^{-1} were found for transect 1 and 2 respectively. Bhatt *et al.* (2010) reported values of 0.001 yr^{-1} and 0.002 yr^{-1} for the East Siberian and Laptev regions respectively, which are the regions in which the transects are located. The trends observed using the longer GIMMS time series could thus also be detected using MODIS 11 years' time series. This proves that, overall, no trend inversion took place for the transects locations between 2000 and 2010, compared to the 1982-2008 period. Trends derived from MODIS even appear to be slightly higher than those derived from the GIMMS dataset. Several hypotheses could potentially explain these differences. The sensitivity of the shorter time series used to an outlying year is supposedly higher than for a nearly 30 years' time series. A single exceptional year could then have created these differences. A second hypothesis is simply that the transects are located in areas where the greening is locally faster than for the considered

Arctic regions as a whole. A last possibility involves an amplification of the greening phenomenon over the last decade, thus resulting in higher trends.

Linear regressions were performed between TI-NDVI trends and SWI trends, and only revealed little to no relation between the two variables. This absence of relationship was unexpected as SWI seems to be an important driver for the establishment of vegetation (cf. relation between average SWI and average TI-NDVI). The fact that the two trends are not correlated does not mean that Arctic greening is not related to climate warming. However, the intensity of the warming does not seem to be determinant in the intensity of the greening. Jia *et al.* (2009) found that there is a nonlinear response of vegetation to climate change and Walker *et al.* (2009) state that many factors, other than temperature change, are likely to affect vegetation greenness. However, whether this lack of relation in the present case is to be attributed to the inertia of plant response to temperature change, to some underlying feedback mechanisms (change in soil activity), or a combination of the two remains uncertain.

As TI-NDVI trend profiles along the two transects were analyzed, we could notice, as expected, a decrease in the intensity of the trend, the farther from the sea, the weaker the trend. This effect seems to happen up to a distance of 120/130 km for transect 2, and 50 km for transect 1. For transect 1, the profile keeps decreasing after the distance of 50 km, but the trend turns negative. The two patterns suggest an effect of the proximity to the sea on the greening trend. However, whether sea ice decline really has an effect on TI-NDVI trends cannot be confirmed from the present study. As presented by Bhatt *et al.* (2010), the effect of sea ice decline on greening is indirect as it enhances the warming first, the latter supposedly affecting vegetation. The theory behind the sea-vegetation relation therefore involves temperature change as a driving factor of vegetation change. Yet from the SWI trend profiles, proximity to the sea does not seem to influence temperature. Furthermore, the results of the regression analyses performed between SWI trends and TI-NDVI trends did not reveal any clear relation between the two variables. As a consequence, even though a potential effect of proximity to the sea on the greening trends could be noticed for both transects, the causality could not be confirmed as it did not happen according to the theory previously proposed to explain the phenomenon.

As mentioned earlier, a local negative vegetation trend could be observed in the case of transect 1. The greening trend turns negative from a distance of 50 km from the north of the transect making it a browning trend for about 100 km. In this section the trend reaches values as low in the negative as the positive local extrema. Detecting such a negative trend at this location was unexpected, and is certainly something to attribute to the use of MODIS relatively fine resolution data, over the coarser GIMMS dataset. Studies like this one, using finer spatial resolutions would not be practical for working on the whole Arctic area. However, they complement the coarser but broader studies well. This transect, in which a local negative trend was detected, is located in the East Siberian Arctic region. An overall positive greening trend was reported for this region by Bhatt *et al.* (2010). Although the reasons for the existence of this negative trend, surrounded by generally greening areas, remain unclear, the phenomenon could have important implications. A region presenting local inversions, as is the case for the area studied, is likely to result in different feedbacks than an area characterized by a homogeneous greening; even if they present the same mean value. Depending on how often the phenomenon occurs, large scale feedbacks of the Arctic may diverge greatly. It is therefore essential for any Arctic study to carefully consider the distribution of the values in addition to the averages. As this phenomenon was detected only for one transect, it is impossible to tell how widespread the phenomenon could be.

Given the importance of Arctic vegetation dynamics for the global climate, further understanding is needed, so that precision can be increased in future climate scenarios. Such fine resolution study should be conducted all over the Arctic and complement the broader and coarser studies conducted. The actual effect of Arctic vegetation change on climate and carbon emissions remains uncertain, but as our understanding of these processes grows, Arctic vegetation evolution should, in the future, be included in permafrost thaw modeling studies, for later predicting Arctic carbon emissions (Blok *et al.*, 2010).

5 Conclusion

This study confirms results found by many studies on the topic of evolution of Arctic vegetation, concluding of a greening trend over the Arctic. A majority of the pixels considered presented positive TI-NDVI trends, hence the greening. Greening detected by nearly 30 years' time series could thus be also detected using shorter, MODIS time series. However, this study brings new insights in the sense that negative TI-NDVI trends could be observed as well, thus bringing browning patches into greening areas. It is not clear what could cause such local decreases, but, depending on how widespread they are, they could have important implications for Arctic feedbacks to the regional and global climates. There is no relation between SWI trends and TI-NDVI trends. It therefore seems that the intensity of the warming does not determine the speed of the greening process. Even though slight patterns could be observed in greening trends, especially in the near shore section of both transects, the theory that proximity to the sea influences the greening process could not be confirmed. The lack of relation between SWI and TI-NDVI trends as well as the fact that no patterns could be observed in the SWI trend profiles rejected the hypothesis. By providing new information on the spatial variations of vegetation through the Arctic, this research should bring new insights to further Arctic vegetation prediction studies, the latter contributing to permafrost thaw modeling studies, and carbon emission predictions associated.

References

Bhatt, U.S., Alexander, M.A., Deser, C., Walsh, J.E., Miller, J.S., Timlin, M.S., Scott, J., Tomas, R.A., 2008. The atmospheric response to realistic reduced summer Arctic sea ice anomalies. Arctic Sea Ice Decline: Observations, Projections, Mechanisms, and Implications. Geophys. Monogr 180, 91–110.

Bhatt, U.S., Walker, D.A., Raynolds, M.K., Comiso, J.C., Epstein, H.E., Jia, G., Gens, R., Pinzon, J.E., Tucker, C.J., Tweedie, C.E., Webber, P.J., 2010. Circumpolar Arctic tundra vegetation change is linked to sea ice decline. Earth Interactions 14.

Blok, D., Heijmans, M.M.P.D., Schaepman-Strub, G., Kononov, A.V., Maximov, T.C., Berendse, F., 2010. Shrub expansion may reduce summer permafrost thaw in Siberian tundra. Global Change Biology 16, 1296-1305.

Chapin, I., F. S., McGuire, A.D., Randerson, J., Pielke Sr, R., Baldocchi, D., Hobbie, S.E., Roulet, N., Eugster, W., Kasischke, E., Rastetter, E.B., Zimov, S.A., Running, S.W., 2000. Arctic and boreal ecosystems of western North America as components of the climate system. Global Change Biology 6, 211-223.

Chapin, I., F. S., Shaver, G.R., Giblin, A.E., Nadelhoffer, K.J., Laundre, J.A., 1995. Responses of Arctic tundra to experimental and observed changes in climate. Ecology 76, 694-711.

Comiso, J.C., Parkinson, C.L., Gersten, R., Stock, L., 2008. Accelerated decline in the Arctic sea ice cover. Geophysical Research Letters 35.

Dutta, K., Schuur, E.A.G., Neff, J.C., Zimov, S.A., 2006. Potential carbon release from permafrost soils of Northeastern Siberia. Global Change Biology 12, 2336-2351.

Epstein, H.E., Walker, D.A., Raynolds, M.K., Jia, G.J., Kelley, A.M., 2008. Phytomass patterns across a temperature gradient of the North American arctic tundra. Journal of Geophysical Research G: Biogeosciences 113.

Eugster, W., Rouse, W.R., Pielke Sr, R.A., McFadden, J.P., Baldocchi, D.D., Kittel, T.G.F., Chapin Iii, F.S., Liston, G.E., Vidale, P.L., Vaganov, E., Chambers, S., 2000. Land-atmosphere energy exchange in Arctic tundra and boreal forest: Available data and feedbacks to climate. Global Change Biology 6, 84-115.

Hansen, J., Ruedy, R., Sato, M., Lo, K., 2010. Global surface temperature change. Reviews of Geophysics 48.

Hill, G.B., Henry, G.H.R., 2011. Responses of High Arctic wet sedge tundra to climate warming since 1980. Global Change Biology 17, 276-287.

Hudson, J.M.G., Henry, G.H.R., 2009. Increased plant biomass in a high arctic heath community from 1981 to 2008. Ecology 90, 2657-2663.

Huete, A., Didan, K., Miura, T., Rodriguez, E.P., Gao, X., Ferreira, L.G., 2002. Overview of the radiometric and biophysical performance of the MODIS vegetation indices. Remote Sensing of Environment 83, 195-213.

Jia, G.J., Epstein, H.E., Walker, D.A., 2009. Vegetation greening in the canadian arctic related to decadal warming. Journal of Environmental Monitoring 11, 2231-2238.

Jönsson, P., Eklundh, L., 2002. Seasonality extraction by function fitting to time-series of satellite sensor data. IEEE Transactions on Geoscience and Remote Sensing 40, 1824-1832.

Jönsson, P., Eklundh, L., 2004. TIMESAT - A program for analyzing time-series of satellite sensor data. Computers and Geosciences 30, 833-845.

Kaufman, D.S., Schneider, D.P., McKay, N.P., Ammann, C.M., Bradley, R.S., Briffa, K.R., Miller, G.H., Otto-Bliesner, B.L., Overpeck, J.T., Vinther, B.M., Abbott, M., Axford, Y., Bird, B., Birks, H.J.B., Bjune, A.E., Briner, J., Cook, T., Chipman, M., Francus, P., Gajewski, K., Geirsddttir, Á., Hu, F.S., Kutchko, B., Lamoureux, S., Loso, M., MacDonald, G., Peros, M., Porinchu, D., Schiff, C., Seppä, H., Thomas, E., 2009. Recent warming reverses long-term arctic cooling. Science 325, 1236-1239.

Olthof, I., Latifovic, R., 2007. Short-term response of arctic vegetation NDVI to temperature anomalies. International Journal of Remote Sensing 28, 4823-4840.

Qi, J., Chehbouni, A., Huete, A.R., Kerr, Y.H., Sorooshian, S., 1994. A modified soil adjusted vegetation index. Remote Sensing of Environment 48, 119-126.

R Development Core Team, 2011. R: A language and environment for statistical computing. R Foundation for Statistical Computing, Vienna, Austria.

Raynolds, M.K., Comiso, J.C., Walker, D.A., Verbyla, D., 2008. Relationship between satellite-derived land surface temperatures, arctic vegetation types, and NDVI. Remote Sensing of Environment 112, 1884-1894.

Reed, B.C., Brown, J.F., Vanderzee, D., Loveland, T.R., Merchant, J.W., Ohlen, D.O., 1994. Measuring phenological variability from satellite imagery. Journal of Vegetation Science 5, 703-714.

Schuur, E.A.G., Bockheim, J., Canadell, J.G., Euskirchen, E., Field, C.B., Goryachkin, S.V., Hagemann, S., Kuhry, P., Lafleur, P.M., Lee, H., Mazhitova, G., Nelson, F.E., Rinke, A., Romanovsky, V.E., Shiklomanov, N., Tarnocai, C., Venevsky, S., Vogel, J.G., Zimov, S.A., 2008. Vulnerability of permafrost carbon to climate change: Implications for the global carbon cycle. BioScience 58, 701-714.

Serreze, M.C., Francis, J.A., 2006. The arctic amplification debate. Clim. Change 76, 241-264.

Stow, D.A., Hope, A., McGuire, D., Verbyla, D., Gamon, J., Huemmrich, F., Houston, S., Racine, C., Sturm, M., Tape, K., Hinzman, L., Yoshikawa, K., Tweedie, C., Noyle, B., Silapaswan, C., Douglas, D., Griffith, B., Jia, G., Epstein, H., Walker, D., Daeschner, S., Petersen, A., Zhou, L., Myneni, R., 2004. Remote sensing of vegetation and land-cover change in Arctic Tundra Ecosystems. Remote Sensing of Environment 89, 281-308.

Sturm, M., McFadden, J.P., Liston, G.E., Stuart Chapin Iii, F., Racine, C.H., Holmgren, J., 2001. Snow-shrub interactions in Arctic Tundra: A hypothesis with climatic implications. Journal of Climate 14, 336-344.

Tucker, C.J., Pinzon, J.E., Brown, M.E., Slayback, D.A., Pak, E.W., Mahoney, R., Vermote, E.F., El Saleous, N., 2005. An extended AVHRR 8-km NDVI dataset compatible with MODIS and SPOT vegetation NDVI data. International Journal of Remote Sensing 26, 4485-4498.

Von Deimling, S.T., Meinshausen, M., Levermann, A., Huber, V., Frieler, K., Lawrence, D.M., Brovkin, V., 2011. Estimating the permafrost-carbon feedback on global warming. Biogeosciences Discussions 8, 4727-4761.

Walker, D.A., Leibman, M.O., Epstein, H.E., Forbes, B.C., Bhatt, U.S., Raynolds, M.K., Comiso, J.C., Gubarkov, A.A., Khomutov, A.V., Jia, G.J., Kaarlejärvi, E., Kaplan, J.O., Kumpula, T., Kuss, P., Matyshak, G., Moskalenko, N.G., Orekhov, P., Romanovsky, V.E., Ukraientseva, N.G., Yu, Q., 2009. Spatial and temporal patterns of greenness on the Yamal Peninsula, Russia: Interactions of ecological and social factors affecting the Arctic normalized difference vegetation index. Environmental Research Letters 4.

Walker, D.A., Reynolds, M.K., Daniëls, F.J.A., Einarsson, E., Elvebakk, A., Gould, W.A., Katenin, A.E., Kholod, S.S., Markon, C.J., Melnikov, E.S., Moskalenko, N.G., Talbot, S.S., Yurtsev, B.A., Bliss, L.C., Edlund, S.A., Zoltai, S.C., Wilhelm, M., Bay, C., Gudjónsson, G., Ananjeva, G.V., Drozdov, D.S., Konchenko, L.A., Korostelev, Y.V., Ponomareva, O.E., Matveyeva, N.V., Safranova, I.N., Shelkunova, R., Polezhaev, A.N., Johansen, B.E., Maier, H.A., Murray, D.F., Fleming, M.D., Trahan, N.G., Charron, T.M., Lauritzen, S.M., Vairin, B.A., 2005. The Circumpolar Arctic vegetation map. Journal of Vegetation Science 16, 267-282.

Walker, M.D., Wahren, C.H., Hollister, R.D., Henry, G.H.R., Ahlquist, L.E., Alatalo, J.M., Bret-Harte, M.S., Calef, M.P., Callaghan, T.V., Carroll, A.B., Epstein, H.E., Jónsdóttir, I.S., Klein, J.A., Magnússon, B., Molau, U., Oberbauer, S.F., Rewa, S.P., Robinson, C.H., Shaver, G.R., Suding, K.N., Thompson, C.C., Tolvanen, A., Totland, Ø., Turner, P.L., Tweedie, C.E., Webber, P.J., Wookey, P.A., 2006. Plant community responses to experimental warming across the tundra biome. Proc. Natl. Acad. Sci. U. S. A. 103, 1342-1346.

Zhou, L., Tucker, C.J., Kaufmann, R.K., Slayback, D., Shabanov, N.V., Myneni, R.B., 2001. Variations in northern vegetation activity inferred from satellite data of vegetation index during 1981 to 1999. J. Geophys. Res. D Atmos. 106, 20069-20083.

Appendix 1: SWI / TI-NDVI relation for transect 1 (top) and transect 2 (bottom)